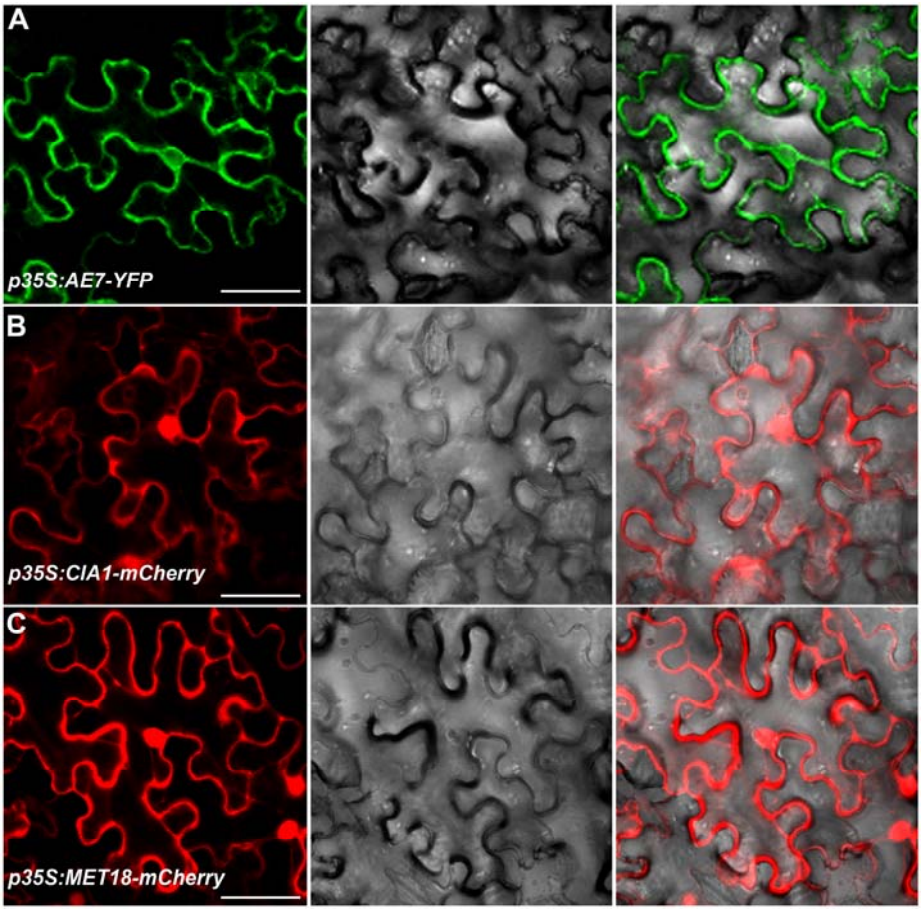

Supplemental Figure 1. Subcellular localization of AE7, CIA1 and MET18.

(A-C) Tobacco leaves were infiltrated with *p35S:AE7-YFP* (A), *p35S: CIA1-mCherry* (B) or *p35S:MET18-mCherry* (C), respectively. AE7-YFP (A), CIA1-mCherry (B) or MET18-mCherry (C) signals were detected in both nuclei and cytoplasm. Bars in (A-C), 50 μm.

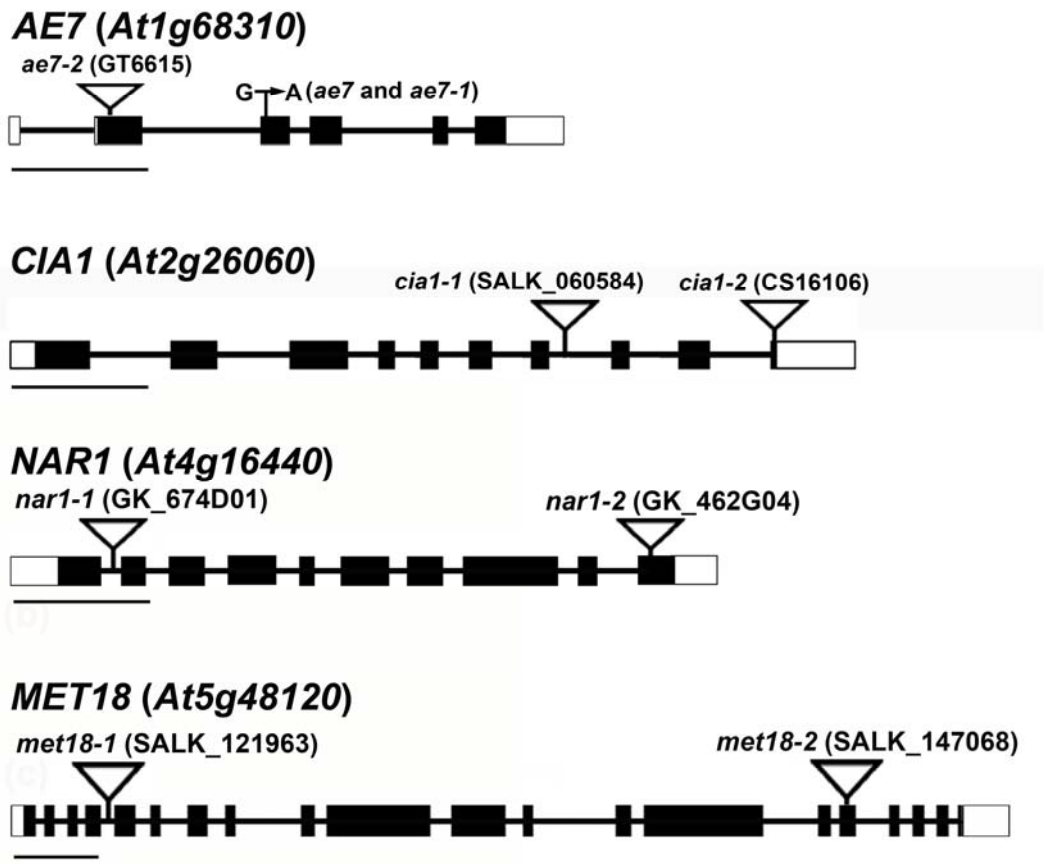

Supplemental Figure 2. Diagram of gene structures of *AE7*, *CIA1*, *NAR1* and *MET18*. Black and white boxes symbolize exons and untranslated regions, respectively, and horizontal lines indicate introns. Triangles show positions where a transposon (in *ae7-2*) or T-DNA (in *cia1-1*, *cia1-2*, *nar1-1*, *nar1-2*, *met18-1*, and *met18-2*) were located in the gene. Bars, 500 bp.

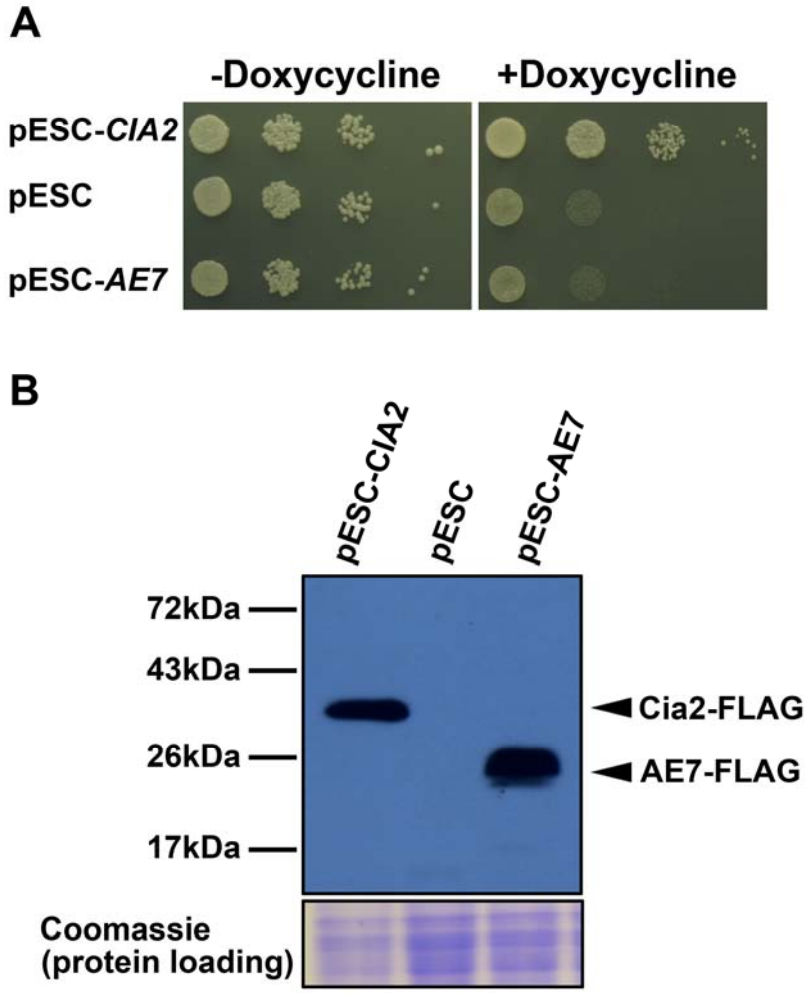

Supplemental Figure 3. *Arabidopsis AE7* failed to rescue the growth of a yeast strain with a doxycycline-repressable *CIA2/YHR122W* gene. (A) The growth of a yeast strain with a doxycycline-repressable *CIA2/YHR122W* gene could not be rescued by expression of the *Arabidopsis AE7* gene. Ten-fold serial dilutions of yeast were grown in the absence (left panel) or presence (right panel) of 10 μg/ml doxycycline that can down-regulate the *CIA2/YHR122W* gene. Cells were transformed with the pESC plasmid containing another copy of the yeast *CIA2* gene fused in-frame with a FLAG-tag (pESC-*CIA2*), and empty plasmid (pESC) or the *Arabidopsis AE7* gene with a FLAG-tag sequence (pESC-*AE7*). (B) Western blot analysis using the Anti-FLAG antibody confirmed the accumulation of Cia2-FLAG and AE7-FLAG proteins.

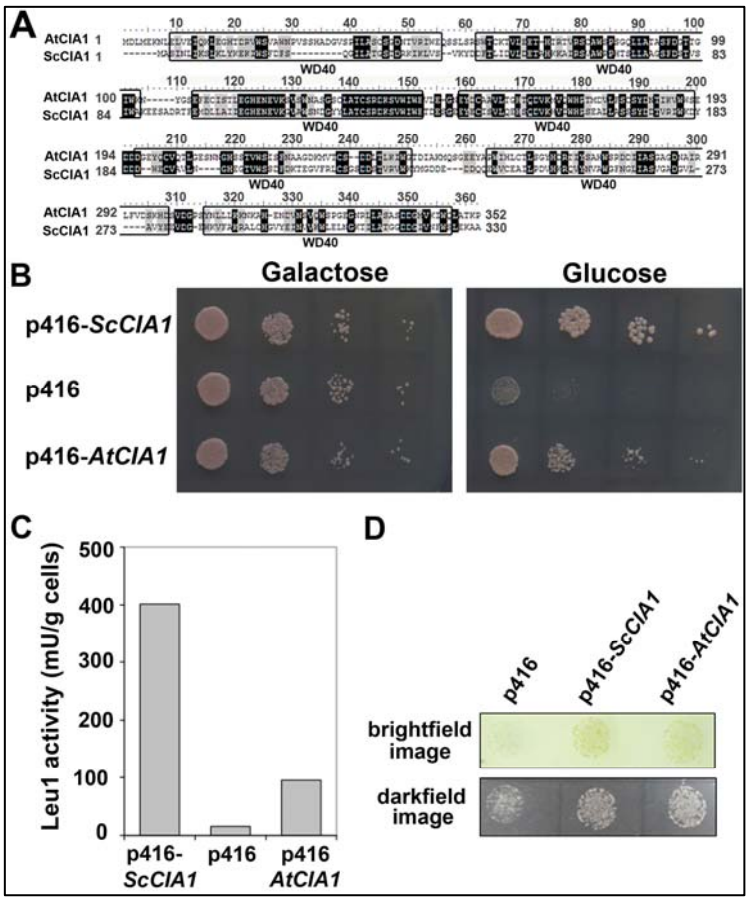

Supplemental Figure 4. *Arabidopsis CIA1* rescued the yeast Gal-*CIA1* mutant. (A) Alignment of the full-length amino acid sequences of AtCIA1 and ScCIA1. (B) The yeast Gal-*CIA1* cells were transformed with the yeast expression vector p416 containing the yeast *CIA1* gene (p416-*ScCIA1*), p416 only, or the coding sequence of *Arabidopsis CIA1* (p416-*AtCIA1*). Cells were grown at 30℃on rich media containing galactose (left) or glucose (right) to induce or repress, respectively, genomic *CIA1* expression. (C) Cell extracts of the transformants described in (B) were analysed for the activity of Leu1, a cytosolic Fe-S enzyme. (D) Cells as in (B) were tested for the activity of sulfite reductase.Yeast was spotted on minimal agar medium with glucose to deplete expression of the genomic copy of *CIA1*. The plate also contained 0.1% (w/v) bismuth ammonium citrate and 0.03% (w/v) sulfite. Sulfite is reduced to sulfide by SiR, a [4Fe-4S] siroheme enzyme, which forms a brown precipitate with bismuth.

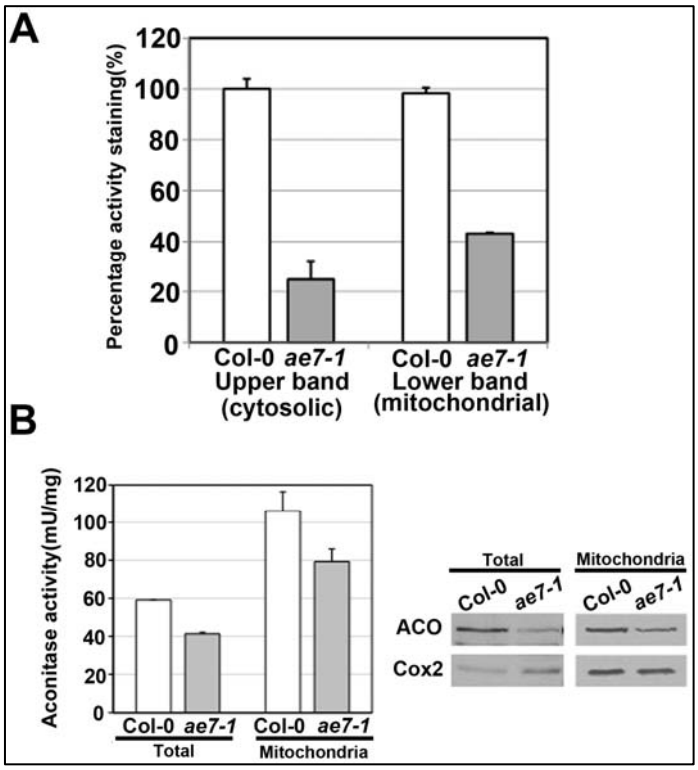

Supplemental Figure 5. Aconitase activity in wild type and *ae7-1* seedlings. (A) Quanification of in-gel aconitase activities. The in-gel activity staining in Figure 6A, top panel, was quantified using ImageJ software. (B) Aconitase activity and protein levels in total extract and purified mitochondria. Total proteins were extracted as for in-gel activity assays, except that hydroponically grown seedlings were used as plant material. Mitochondria were purified from 14-day old hydroponic seedlings, using differential centrifugation and Percoll gradients, as described previously (Sweetlove et al., 2007). Aconitase activity was measured as NADPH production in a coupled assay with isocitrate dehydrogenase. The same protein fractions were subjected to immunoblotting with specific antibodies against aconitase and Cox2. Cox2 is a subunit of Complex IV and serves as a mitochondrial marker.

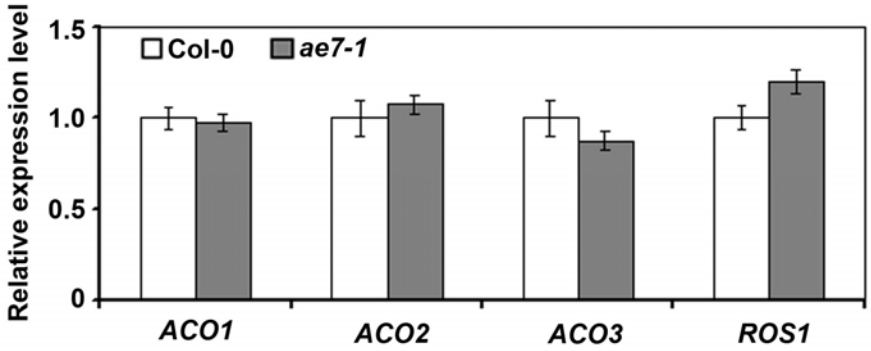

Supplemental Figure 6. qRT-PCR analysis of expressions of the *ACO* and *ROS1* genes. Total RNA prepared from 14-day-old seedlings was amplified by RT-PCR. All values were normalized against the expression level of the *ACTIN* genes. Triplicate repeats and three biological replicates were performed and the data are shown as the averages with s.d.

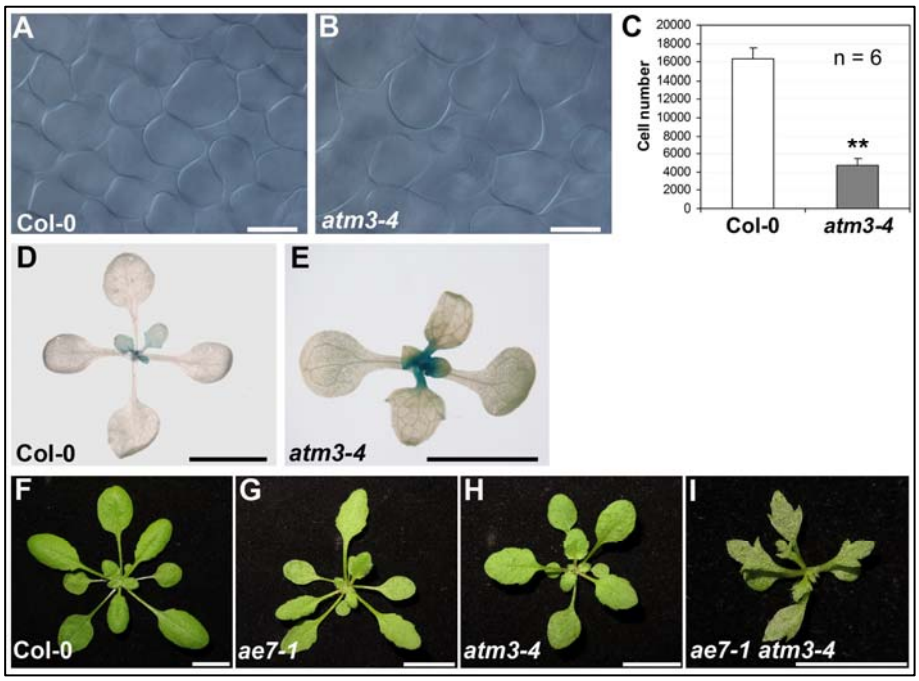

Supplemental Figure 7. The *atm3-4* mutant showed cell proliferation defects and a genetic interaction with *ae7-1*. (A-C) Compared with the wild type (A), the size of palisade cells in the first rosette leaf from 25-day-old *atm3-4* seedlings (B) is enlarged, while the number of palisade cells in *atm3-4* leaves is reduced (C). * Significant statistical differences by t-test ($P < 0.01$). (D, E) Histochemical localization of GUS activity in the shoot apex of 13-day-old wild type (D) and *atm3-4* (E) seedlings harboring the CYCB1;1:GUS reporter, respectively. (F-I) Genetic interaction between *ae7-1* and *atm3-4*. Compared with the wild type (F) or *ae7-1* (G) and *atm3-4* (H) single mutants, the *ae7-1 atm3-4* double mutant (I) exhibited enhanced developmental defects, including a diminutive plant size and serrated leaves. Bars in (A, B), 50μm; in (D, E), 0.5cm; in (F-I), 1 cm.

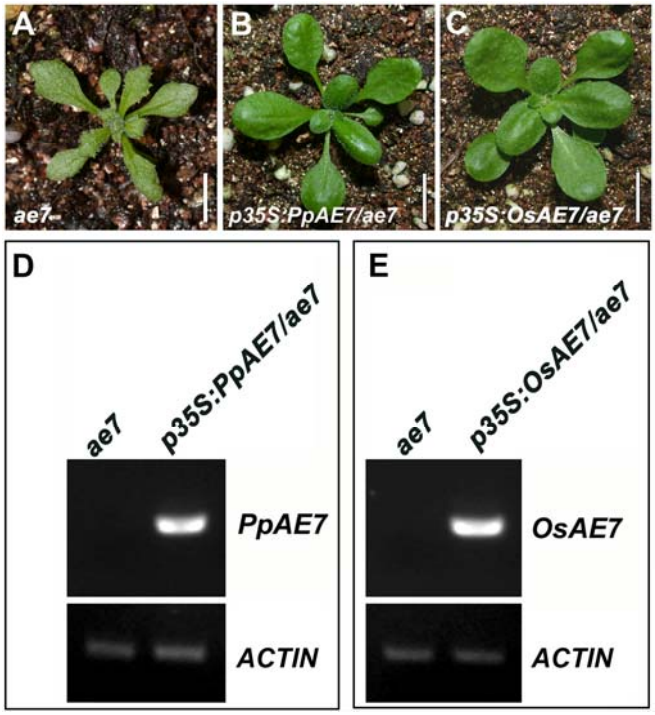

Supplemental Figure 8. The *ae7* phenotype was rescued by the moss (*Physcomitrella patens*) and rice (*Oryza sativa*) orthologues of *AE7*. (A) The *ae7* mutant. (B, C) The *ae7* mutant transformed with the *Physcomitrella patens* Pp-*AE7* (B) and rice Os-*AE7* (C). (D, E) RT-PCR to analyze the transcripts of the Pp-*AE7* and Os-*AE7* in the corresponding transgenic plants. Bars in (A-C), 1 cm.

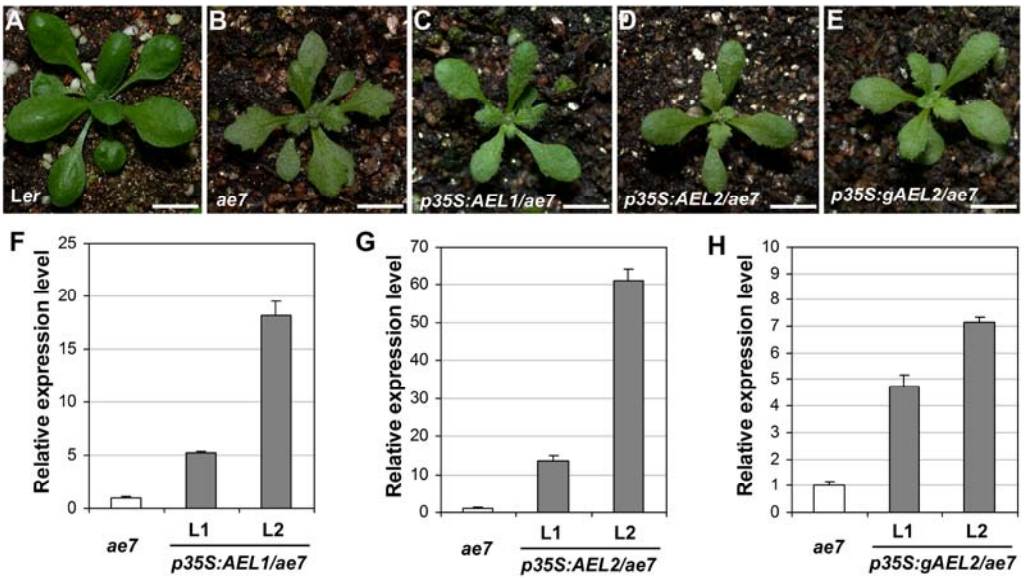

Supplemental Figure 9. The *ae7* phenotype could not be rescued by *Arabidopsis AE7*-like genes, *AEL1* (*At3g50845*) and *AEL2* (*At3g09380*), respectively. (A) The wild-type L*er*. (B) The *ae7* mutant. (C-E) The representative transgenic *ae7* plant expressing the *AEL1* coding region (C), *AEL2* coding region (D) or *AEL2* genomic fragment (E) driven by the *p35S* promoter. (F-H) qRT-PCR analysis of *AEL1* (F) and *AEL2* expression (G, H) in the corresponding transgenic plants. Bars in (A-E), 1 cm.

Supplemental data. Luo et al. Plant Cell. (2012). 10.1105/tpc.112.102608

Supplemental Table 1. Sequences of oligonucleotide primers used in this study.

Name	Gene or mutant	Sequence (5'-3')	Purpose
ACTIN-F	*ACTIN*	TGGCATCA(T/C)ACTTTCTACAA	qPCR
ACTIN-R	*ACTIN*	CCACCACT(G/A/T)AGCACAATGTT	qPCR
BRCA1-realF	*BRCA1*	CCATGTATTTTGCAATGCGTG	qPCR
BRCA1-realR	*BRCA1*	TGTGGAGCACCTCGAATCTCT	qPCR
RAD51-realF	*RAD51*	CGAGGAAGGATCTCTTGCAG	qPCR
RAD51-realR	*RAD51*	GCACTAGTGAACCCCAGAGG	qPCR
PARP1-realF	*PARP1*	TGCTCGCGCGAACTCACTTCT	qPCR
PARP1-realR	*PARP1*	AGCCTCTCCACCAGAACGGCT	qPCR
PARP2-realF	*PARP2*	ATGGCGTTCTGCTCCTCTGC	qPCR
PARP2-realR	*PARP2*	GGTGCTGTTTTCCCCACACC	qPCR
WEE1-realF	*WEE1*	TGGTGCTGGACATTTCAGTCGG	qPCR
WEE1-realR	*WEE1*	CAAGAGCTTGCACTTCCATCATAG	qPCR
CYCB1;1-F	*CYCB1;1*	CAGACCATGCATACAGTCAC	qPCR
CYCB1;1-R	*CYCB1;1*	TCCTAACTCCTAAGCAGATTC	qPCR
GR1-RTF	*GR1*	GAAGGAGCAGACAAAGTGAG	qPCR
GR1-RTR	*GR1*	GGTGAGATGGAAGTGATAGG	qPCR
LIG4-RTF	*LIG4*	GGTGGTCTCAATGTTCACCGCCC	qPCR
LIG4-RTR	*LIG4*	AGGTCAGCACCAGCCCGGAT	qPCR
KU70-RTF	*KU70*	CGAGGACGACGTTGCAGAGAGC	qPCR
KU70-RTR	*KU70*	GCTGCCAGGAATAGCCGGACG	qPCR
KU80-RTF	*KU80*	GATGATGAAGACAATCGCATGATTA	qPCR
KU80-RTR	*KU80*	TTAGCTCTCGAGCATTGACTC	qPCR
RNR2A-RTF	*AtRNR2A*	TGGCTCAGAACCAGAGATTC	qPCR
RNR2A-RTR	*AtRNR2A*	AGAAACTGGCTTCAGCCTTC	qPCR
TSO2-RTF	*AtTSO2*	TCGCTTGTCTACTCTACACG	qPCR
TSO2-RTR	*AtTSO2*	CCGCGTCGCAGACGATTGA	qPCR
RNR2B-RTF	*AtRNR2B*	CTGGACAGCCGAAAAGTC	qPCR
RNR2B-RTR	*AtRNR2B*	AGTGACGTTCGTCGTTGGTT	qPCR
ACO1-F	*ACO1*	CATTGAGCTCCCAAACAATGTTAGT	qPCR
ACO1-R	*ACO1*	TTATTGTTTGATCAAGTTCCTG	qPCR
ACO2-F	*ACO2*	ATGCCACCTTCCTACAAAAGTTAGT	qPCR
ACO2-R	*ACO2*	ATCACTTGGCGCTCAAACTCC	qPCR
ACO3-F	*ACO3*	GATCCATCTCCCAACCGATATCTCA	qPCR
ACO3-R	*ACO3*	CTATTGCTTGCTCAAGTTTCTG	qPCR
ROS1-F	*ROS1*	GGATCATGCATCCAGCCTAAACC	qPCR
ROS1-R	*ROS1*	TTAGGCGAGGTTAGCTTGTTGTC	qPCR
AEL1-RT-F	*AEL1*	CCGGAATTCATGACTCTGGGACTGAT AAACG	qPCR
AEL1-RT-R	*AEL1*	GACTAGTGCTATCTCATCGGAGTAGAT AC	qPCR
AEL2-RT-F	*AEL2*	CCGGAATTCATGCGTTCAGGAGAGA	qPCR

AEL2-RT-R	*AEL2*	GACTAGTGCAGATGCAAAGACCAATA TG	qPCR
Salk_060584-F	*atcia1-1*	GACAAGATGGTCACTTGTAG	T-DNA
Salk_060584-R	*atcia1-1*	GATTATATGAAGGTCCATCAAC	T-DNA
CS16106-F	*atcia1-2*	CTGAAGAAGAATAAAGCACATG	T-DNA
CS16106-R	*atcia1-2*	GCACCATCTAGCTTTCAACTCC	T-DNA
Salk_121963-F	*atmet18-1*	CTTTGGAGAATGATTCTTTATC	T-DNA
Salk_121963-R	*atmet18-1*	CATAGCATAAACAAGTAGATCAC	T-DNA
Salk_147068-F	*atmet18-2*	GAATTCCCAGACTTCACTATCGAG	T-DNA
Salk_147068-R	*atmet18-2*	CATTAGATGCGGATATGATGTAAG	T-DNA
GK_674D01-F	*atnar1-1*	TGGTACCGAATTCATGTCAGAGA AGT TTTCACC GAC	T-DNA
GK_674D01-R	*atnar1-1*	GATCGCAGCTCCAATAGCTTGCTG	T-DNA
GK_462G04-F	*atnar1-2*	GAGATCTTTATGGTGTAGCTGGGAG	T-DNA
GK_462G04-R	*atnar1-2*	GTCGACGGATCCCCAGTTGTTGAGCT GCGACGTA	T-DNA
GT6615-F	*ae7-2*	GAGGTTACACAGACCTACTCCTC	DS-Transposon
GT6615-R	*ae7-2*	CCGCTCGAGCGGTCACTCTTCTGATG GCAGGCATTC	DS-Transposon
XBAT34-F	*XBAT34*	GTTTGAAGCATATCTCCTCTATG	McrBC-PCR
XBAT34-R	*XBAT34*	AGGTCGTTATTTGTTCATCGGTG	McrBC-PCR
MRD1-F	*MRD1*	GTCCGTTTTAGGCTTAGGACCG	McrBC-PCR
MRD1-R	*MRD1*	GAAAACATTTCTAGCACAAAGAAA	McrBC-PCR

Supplemental References

Sweetlove, L.J., Taylor, N.L., and Leaver, C.J. (2007). Isolation of intact, functional mitochondria from the model plant *Arabidopsis thaliana*. Methods Mol. Biol. **372:** 125-136.